Extraction of Cu(II) From Acidic Sulfate Media by Palm Kernel Fatty Acid Distillate: Stoichiometry and Thermodynamic Studies

siti fatimah abdul halim
Universiti Teknologi MARA - Kampus Pulau Pinang https://orcid.org/0000-0003-1662-5374
Norhashimah Morad
Universiti Sains Malaysia
Siu Hua Chang (shchang@uitm.edu.my)
Universiti Teknologi MARA - Kampus Pulau Pinang

Research Article

Keywords: Stoichiometry, Cu(II), free fatty acids, palm kernel fatty acid distillate, extraction thermodynamics

Posted Date: June 7th, 2021

DOI: https://doi.org/10.21203/rs.3.rs-549474/v1

Extraction of Cu(II) from acidic sulfate media by palm kernel fatty acid distillate: stoichiometry and thermodynamic studies

Siti Fatimah Abdul Halim[ab], Norhashimah Morad[c] and Siu Hua Chang[ab]*,

[a]Faculty of Chemical Engineering, Universiti Teknologi MARA (UiTM), Cawangan Pulau Pinang, 13500 Permatang Pauh, Pulau Pinang, Malaysia.

[b]Faculty of Chemical Engineering, Universiti Teknologi MARA (UiTM), 40450 Shah Alam, Malaysia

[c]School of Industrial Technology, Universiti Sains Malaysia, 11800 Pulau Pinang, Malaysia.

*Corresponding author: shchang@uitm.edu.my

Abstract

In efforts to develop a novel low-cost and eco-friendly organic solvent, namely, palm kernel fatty acid distillate (PKFAD), with free fatty acids (FFAs) as the active components, for Cu(II) extraction from acidic sulfate media, this work aimed to gain insight into the stoichiometry of Cu(II)-FFA complexes (extracted species) in PKFAD and their extraction thermodynamics. The former was explored by both the equilibrium slope and numerical analyses, while the latter was determined from the extraction of Cu(II) by PKFAD at different temperatures. Both the equilibrium slope and numerical analyses revealed that the stoichiometry of Cu(II)-FFA complexes in PKFAD was 1:6, whereas the thermodynamic study indicated that Cu(II) extraction by PKFAD was exothermic, nonspontaneous, and enthalpy-driven over the temperature range studied. A plausible structure of Cu(II)-FFA complexes in PKFAD was also postulated based on the thermodynamic data obtained.

Keywords: *Stoichiometry*; *Cu(II); free fatty acids; palm kernel fatty acid distillate; extraction thermodynamics*

1.0 Introduction

Copper, an element located in the d-block of the periodic table, is a soft, malleable, and ductile transition metal with remarkable thermal and electrical conductivity, good corrosion resistance, and antimicrobial properties (Michels et al., 2008). It finds broad applications in various industries (e.g. metallurgical, electroplating, electrical and electronics, automotive, construction, telecommunications, and healthcare (Chang, 2018; Gopi Kiran et al., 2017)) and is mined mainly from oxide and sulfide ores using sulfuric acid as a lixiviant (Bar and Barkat, 2016; Wang, 2007). With a finite supply of copper from the ground and the increasing demand for copper in the global market, it is essential to recover copper more efficiently.

Solvent extraction is an established and widely used separation method for recovering metal ions from aqueous media due to its simplicity, rapidity, ability to operate in a wide range of concentrations, and high recovery and selectivity (Rydberg et al., 2004). However, metal ions exist as hydrated ions in aqueous media that have little, or no, inclination to transfer to an organic phase. To achieve the required transfer, modification of metal ions into an extractable species which carry neutral charges and possess little, or no, water of hydration is necessary. This can be accomplished with the aid of an extractant via the cation exchange, ion-pairing or hydrated water replacement mechanism (Wilson et al., 2014).

The development of an efficient extractant for a metal ion requires the fundamental understanding of the stoichiometry of the metal-extractant complexes (extracted species) formed and their extraction thermodynamics. The stoichiometry provides the precise number

of moles of each substance required to form one mole of metal-extractant complexes under favorable thermodynamic conditions, while the thermodynamics explains the extraction behavior of a metal ion by the extractant (Choppin and Morgenstern, 2000; Wahab et al., 2016). The stoichiometry of various metal-extractant complexes in different diluents have been reported, for instance, 1:4 and 1:2 for Cu(II)-di-2-ethylhexylphosphoric acid (D2EHPA) complexes in soybean oil (Chang et al., 2011) and waste palm cooking oil (Wahab et al., 2016), respectively; 1:2 for Cu(II)-2-hydroxy-5-nonylacetophenone oxime (active component of LIX 84) complexes in toluene (Elizalde et al., 2019); 1:6 for Nd(III)-D2EHPA complexes in sulfonated kerosene (Yin et al., 2015); 1:3 for Ga(III)-hexaacetato calix(6)arene in xylene (Thakare and Malkhede, 2014); and 1:2 for hydrated Ni(II)-dinonylnaphthalene disulfonic acid and 2-ethylhexyl 4-pyridinecarboxylate ester complexes in sulfonated kerosene (Hu et al., 2018). The majority of these works used either the equilibrium slope or numerical analysis, or both, to determine the stoichiometry of metal-extractant complexes (Chang et al., 2011; Elizalde et al., 2019; Thakare and Malkhede, 2014; Wahab et al., 2016; Yin et al., 2015). Other methods like the Job plot (Wahab et al., 2016) and quantitative analysis with FTIR (Chang et al., 2011) had also been applied. Meanwhile, various thermodynamic parameters, namely, the standard enthalpy change (ΔH^o), standard entropy change (ΔS^o), and standard Gibbs free energy change (ΔG^o) of several metal-extractant complexes in different diluents have also been recorded, for instance, ΔH^o of 35.40 and 30.05 kJ·mol^{-1}, ΔS^o of -0.011and -0.016 kJ·mol^{-1}·K^{-1}, and ΔG^o of 38.80 and 34.56 kJ·mol^{-1} for Cu(II)-capric acid (Aidi and Barkat, 2018) and Cu(II)-*N*-(2 hydroxybenzylidene) aniline (Aidi and Barkat, 2010) complexes, respectively, in cyclohexane; ΔH^o of 25.65 kJ·mol^{-1}, ΔS^o of 0.079 kJ·mol^{-1}·K^{-1}, and ΔG^o of 0.86 kJ·mol^{-1} for Zn(II)-D2EHPA complexes in kerosene (Jafari et al., 2018); and ΔH^o of 17.32 kJ·mol^{-1}, ΔS^o of 0.041 kJ·mol^{-1}·K^{-1}, and ΔG^o of 5.09 kJ·mol^{-1} for vanadium(V)-D2EHPA complexes in kerosene (Razavi et al., 2018).

Recently, there is an increasing trend towards the utilization of green organic solvents in solvent extraction for resource recovery following the growing public awareness of environmental issues (Chang, 2020). In this regard, our research team has successfully used a processing residue from palm kernel oil refinery, namely, palm kernel fatty acid distillate (PKFAD), as a novel low-cost and environmentally benign organic solvent for Cu(II) extraction from acidic sulfate media (Halim et al., 2020, 2019). PKFAD is a lipid material with a high free fatty acid (FFA) content of 92 wt% (Halim et al., 2020). We had previously found that FFAs were the active components of PKFAD that extracted up to 98% of Cu(II) from acidic sulfate media by a cation exchange mechanism (Halim et al., 2019). The effects of various extraction parameters on Cu(II) extraction by PKFAD had been investigated, along with the optimum extraction conditions, and the loading capacity and reusability of PKFAD (Halim et al., 2019). The most suitable type and concentration of stripping agent for Cu(II) stripping from Cu(II)-loaded PKFAD had also been determined (Halim et al., 2019). Herein, the stoichiometry of Cu(II)-FFA complexes (extracted species) in PKFAD and their extraction thermodynamics were explored. The former was investigated by both the equilibrium slope and numerical analyses, while the latter was determined from the extraction of Cu(II) by PKFAD over a range of temperatures.

2.0 Experimental Study

2.1 Materials

PKFAD was supplied by a local vendor, i.e., Sime Darby Sdn. Bhd., and was used directly without further purification. Some of physicochemical properties of PKFAD used in this research are provided in Table 1. Copper sulfate pentahydrate ($CuSO_4.5H_2O$) (Merck, ≥ 99.6% purity), kerosene (Pure Chemical, 100% purity), sodium sulfate (Na_2SO_4) (Qrec, ≥

99% purity), sodium hydroxide (NaOH) (Qrec, ≥ 99% purity), and sulfuric acid (H_2SO_4) (Merck, ≥ 98% purity) were used as received.

Table 1 Physicochemical properties of PKFAD

Physicochemical properties	
Density @ 70°C (g/cm^3)	0.89
Viscosity @ 50°C (mPa.s)	23.0
Fatty acid (C:D[a]) composition (wt%)	
Octanoic acid (8:0)	4.5
Decanoic acid (11:0)	3.7
Lauric acid (12:0)	49.1
Myristic acid (14:0)	17.0
Palmitic acid (16:0)	10.0
Stearic acid (18:0)	2.3
Oleic acid (18:1 cis)	11.0
Linoleic acid (18:2 cis)	1.6
FFA (wt%)	92.2

[a]C:D = number of carbon atoms: number of double bonds

2.2 Preparation of aqueous and organic phases

Aqueous phases with various initial Cu(II) concentrations (20, 100, 300, and 500 mg/L) were prepared by dissolving appropriate amounts of $CuSO_4.5H_2O$ in distilled water loaded with 200 mM Na_2SO_4, while the organic phases with different concentrations (0.46-1.87 M) of dimeric FFAs were prepared by using pure PKFAD (containing 1.87 M dimeric FFAs) and by diluting suitable amounts of pure PKFAD with kerosene (inert diluent).

2.3 Extraction procedure

The extraction of Cu(II) ions was performed based on the shake-out test as delineated in our previous work (Halim et al., 2020, 2019). Initially, 15 ml of PKFAD was mixed with a prepared aqueous solution at 0.5:1 organic to aqueous volume ratio in a glass-stoppered conical flask. The flask was then agitated in an incubator shaker (Lab Companion, SI-300) at 150 rpm for 8 min, followed by 5 min settling of the mixture for phase separation. Next, about 8 ml sample was taken from the aqueous phase with a syringe and the equilibrium pH (pH_{eq}) of the sample was measured with a pH meter (Hanna Instruments, HI11310). If the desired pH_{eq} (2.40-4.70) was not obtained, a few drops of 1 M H_2SO_4 or 1 M NaOH were added to the mixture and the mixture was mixed for another 8 min. This step was repeated until the desired pH_{eq} was obtained. Finally, the mixture was transferred into a separating funnel for overnight phase disengagement and about 10 ml sample was withdrawn from the aqueous phase for chemical analysis with a flame atomic absorption spectrometer (Shimadzu, AA7000). The distribution coefficient (D) of Cu(II) was calculated by:

$$D = \frac{[Cu(II)-FFA]_{org}}{[Cu(II)]_{aq}} \quad (1)$$

where $[Cu(II)\text{-}FFA]_{org}$ and $[Cu(II)]_{aq}$ are the concentrations of Cu(II)-FFA complex and Cu(II) in the organic and aqueous phases, respectively, when the extraction reaction reaches equilibrium. All experiments were performed in duplicate or triplicate at room temperature (25°C) unless stated otherwise, and the relative standard deviation between replicate samples within an experiment range was less than 5%.

3.0 Results and Discussion

3.1 Stoichiometry of Cu(II)–FFA complexes in PKFAD

Two of the most prevalent methods to determine the stoichiometry of metal-extractant complexes in organic solvents are the equilibrium slope (Aksamitowski et al., 2019; Ghosh et al., 2018; Sulaiman and Othman, 2018) and numerical analyses (Chang et al., 2011). The former is a graphical method where the stoichiometry of metal-extractant complexes is estimated from the slopes of experimental plots, while the latter involves a multiple regression analysis where the stoichiometry of metal-extractant complexes is evaluated from the best least-squares fit to the experimental data. In this work, both the equilibrium slope and numerical analyses were used to determine the stoichiometry of Cu(II)-FFA complexes in PKFAD.

3.1.1 Equilibrium slope analysis

Being a carboxylic acid, FFA tends to form dimers through hydrogen bonding of the acidic hydrogen and the carbonyl oxygen between two acid molecules (Tsivintzelis et al., 2017). Hence, the extraction of Cu(II) by FFAs (extractants) contained in PKFAD can be expressed as (Benalia and Barkat, 2020):

$$Cu_{aq}^{2+} + \frac{2+m}{2}(HR)_{2,org} \overset{K_{ex}}{\longleftrightarrow} (CuR_2(HR)_m)_{org} + 2H_{aq}^{+} \quad (2)$$

where the subscripts *aq* and *org* correspond to the aqueous and organic phases, respectively, $(HR)_2$ represents the dimeric form of FFA molecules, m is a stoichiometric constant, $CuR_2(HR)_m$ is the Cu(II)-FFA complex formed, and K_{ex} is the equilibrium constant of the reaction. Assuming ideal behavior in both organic and aqueous phases, K_{ex} is given by:

$$K_{ex} = \frac{[CuR_2(HR)_m]_{org}[H^+]_{aq}^2}{[Cu^{2+}]_{aq}[(HR)_2]_{org}^{\frac{2+m}{2}}} \quad (3)$$

Replacing [Cu(II)-FFA]$_{org}$ and [Cu(II)]$_{aq}$ in Eq. (1) with $[CuR_2(HR)_m]_{org}$ and $[Cu^{2+}]_{aq}$, respectively, and substituting it into Eq. (3) yield the following equation correlating D with K_{ex}:

$$D = \frac{K_{ex}[(HR)_2]_{org}^{(2+m)/2}}{[H^+]_{aq}^2} \quad (4)$$

By taking the logarithm of both sides of Eq. (4), it follows that:

$$log\ D = log\ K_{ex} + \frac{2+m}{2} log[(HR)_2] + 2pH_{eq} \quad (5)$$

Fig. 1 shows the plots of log D versus pH_{eq} at various initial Cu(II) concentrations (20, 100, 300 and 500 mg/L). The slope values of about 2 obtained for all initial Cu(II) concentrations studied support the valency of Cu(II) and, thus, the conformity of the experimental data to the theoretical model (Eq. 5). To determine the value of m in Eq. (5), log D is plotted against log $[(HR)_2]$ as shown in Fig. 2. In this investigation, the concentration of dimeric FFAs in PKFAD was varied in the range of 0.46–1.87 M and the extraction experiments were carried out at an initial Cu(II) concentration of 100 mg/L and pH_{eq} of 4.0. The slope value of 3.056 (Fig. 2) corresponds to (2 + m)/2 from Eq. (5), which brings about an m value of ~4. Substituting m = 4 into Eq. (2), Eq. (6) is obtained as follows:

$$Cu_{aq}^{2+} + 3(HR)_{2,org} \overset{K_{ex}}{\longleftrightarrow} (CuR_2(HR)_4)_{org} + 2H_{aq}^+ \quad (6)$$

183 which suggests that one mole of Cu (II) is solvated with three moles of dimeric FFAs, giving
184 rise to a stoichiometric ratio of Cu(II) to FFA of 1:6 in the formation of $CuR_2(HR)_4$ (Cu(II)-
185 FFA) complexes.
186

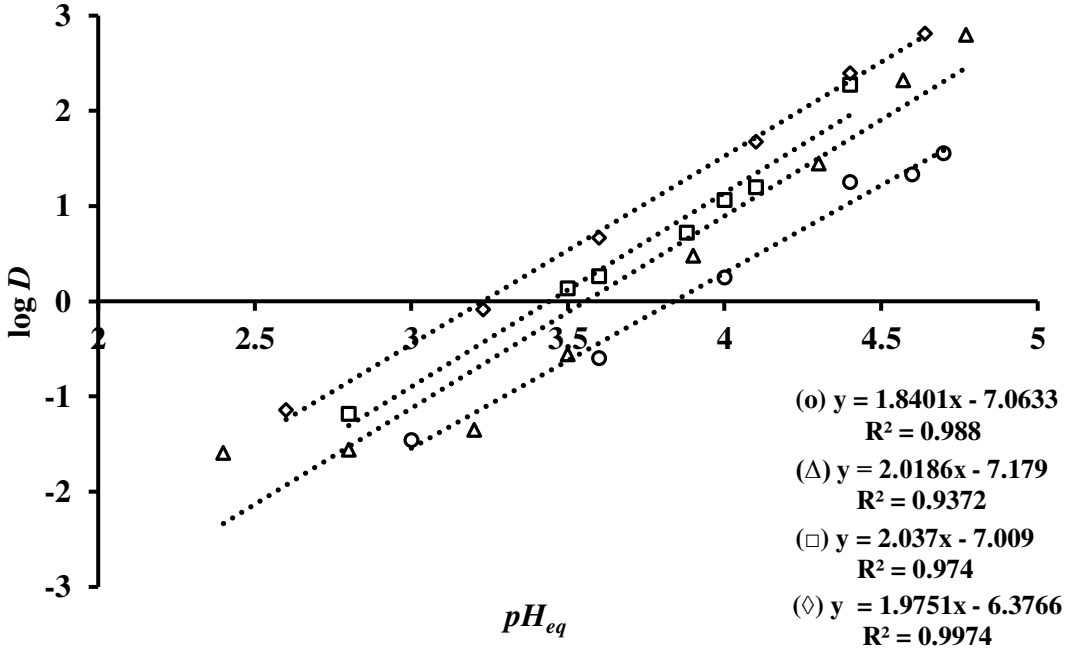

187
188
189 **Fig. 1** log *D* vs. pH_{eq} at different initial Cu(II) concentrations (20 mg/L (○),100mg/L (Δ), 300
190 mg/L (□) and 500 mg/L(◊)
191

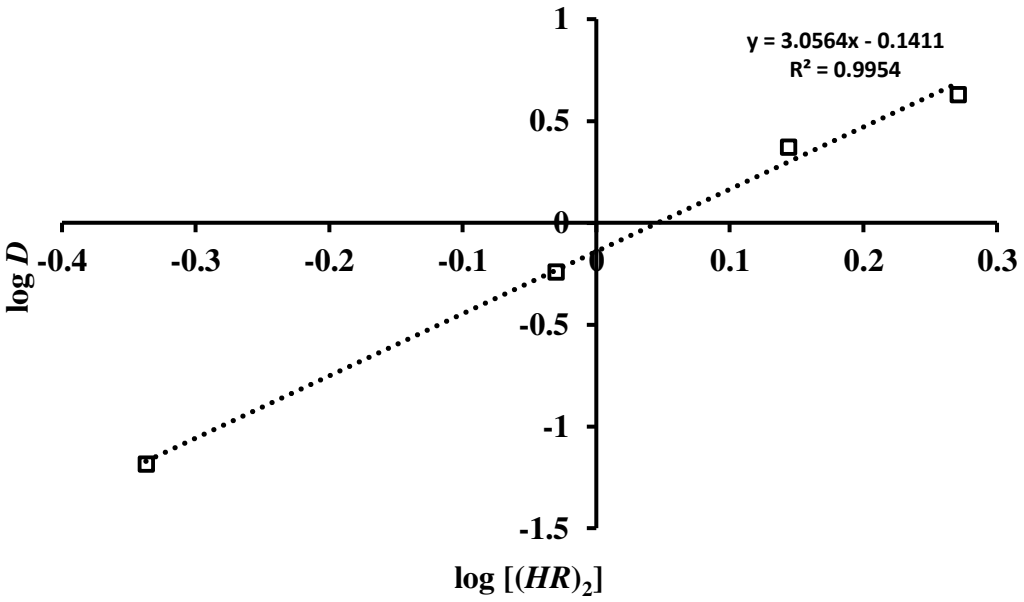

192

193 **Fig. 2** log *D* vs. log [*(HR)*$_2$] at initial Cu(II) concentration of 100 mg/L and pH_{eq} of 4.0

194

195 ***3.1.2 Numerical analysis***

196 The experimental data obtained under an initial Cu(II) concentration of 100 mg/L at
197 various pH_{eq} (Fig. 1) and extractant concentrations (Fig. 2) were fit to run a multiple linear
198 regression analysis using the following first-order polynomial equation (Myers et al., 2016):

199

200 $$y = \beta_o + \sum_{i=1}^{k} \beta_i x_i + \varepsilon \quad (7)$$

201

202 where β_o and β_i are the coefficients for intercept and linear variables, respectively, y is the
203 dependent variable, x_i is the independent variable, and ε is the error term. In this analysis, the
204 dependent variable was log *D* while the independent variables were log *(HR)*$_2$ and pH_{eq}. The
205 coefficients that caused Eq. (7) to best fit the experimental data were estimated by the least-
206 squares method (Myers et al., 2016). All analyses were conducted using Microsoft Excel's
207 (Microsoft Office 2016) at 5% significance level. Table 2 shows the estimated coefficients
208 along with the standard errors, *t*-statistics, and probability (*P*) values for the variable terms

(intercept, log $(HR)_2$, and pH_{eq}) of a regression model for log *D*. Since the *P* values of all variable terms are less than 0.05 at 5% significance level, they are considered statistically significant. Hence, a first-order polynomial model correlating log *D* with all the variable terms could be written as:

$$log\ D = -9.19 + 3.22\ log[(HR)_2] + 2.27\ pH_{eq} \quad (8)$$

Table 2 Estimated coefficients of the regression model for log *D* (Eq. 8)

	Coefficients	SE	*t*-stat	*P*
Intercept	-9.19	0.598	-15.380	0.0000
log $(HR)_2$	3.22	0.389	8.284	0.0000
pH_{eq}	2.27	0.151	15.049	0.0000

SE: standard error; *t*-stat: *t*-statistics; *P*: probability value

The goodness of fit of the regression model (Eq. 8) was examined by the analysis of variance (ANOVA) at 5% significance level and the results are tabulated in Table 3. The high *F* (*F* > *F*-critical of 4.74) and low *P* (*P* < 0.05) values imply that the regression model is significant statistically (Chang et al., 2011). The high coefficient of determination (R^2) of 0.9735, on the other hand, indicates that the sample variation of 97.35% for log *D* is ascribed to the independent variables (pH_{eq} and log $(HR)_2$) of the model and only 2.65% of the total variations are not explained by the model. The small difference (0.78%) between R^2 of 0.9735 and $R^2(adj)$ of 0.9659 suggests that there is a slight chance for the inclusion of any insignificant terms in the model and the model is highly significant (Myers et al., 2016). Fig. 3 shows the plot of the experimental log *D* against the predicted log *D*. Since the great majority of the points fall directly on a straight line, with a high R^2 of 0.9735, the experimental log *D* is said to exhibit an excellent linear relationship with the predicted log *D*.

231 This finding lends support to the fact that the model is capable of giving a reasonably good
232 estimate of log *D* for the system under consideration in the range studied.

233

234 **Table 3** ANOVA of the regression model for log *D* (Eq. 8)

	DF	SS	MS	*F*	*F*-critical	*P*
Regression	2	13.8741	6.9370	128.6364	4.74*	0.0000
Residual	7	0.3775	0.0539			
Total	9	14.2526				

235 DF: degree of freedom; SS: sum of square; MS: mean sum of squares

236 **F*-critical (2,7) at 5% significance level

237 $R^2 = 0.9735$; $R^2(adj) = 0.9659$

238

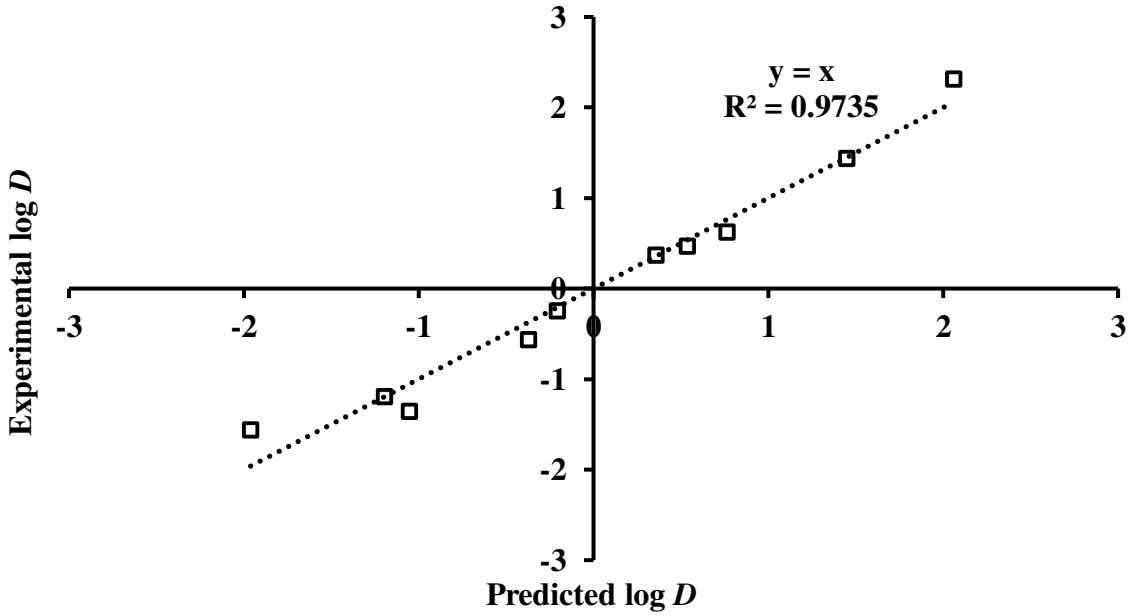

239

240 **Fig. 3** Experimental log *D* vs. predicted log *D*

241

242 Since Eqs. (5) and (8) take the same form, their coefficients for each variable term can
243 be compared conveniently. The close proximity between their coefficients of pH_{eq}, i.e. 2 (Eq.
244 5) vs. 2.27 (Eq. 8), implies that they are fairly compatible. By equating the coefficient of log
245 $[(HR)_2]$ from Eq. (5), i.e., $(2+m)/2$, with that from Eq. (8), an m value of 4.44 ~ 4 is
246 computed, leading to a stoichiometric ratio of Cu(II) to FFA of 1:6 in the formation of
247 $CuR_2(HR)_4$ complexes and this is in good agreement with that obtained earlier in the
248 equilibrium slope analysis (Eq. 6). Nevertheless, this finding contradicts the stoichiometry of
249 1:4 for Cu(II)-FFA complexes in chloroform (F.Adjel and D.Barkat, 2011), cyclohexane
250 (Guerdouh and Barkat, 2015), and toluene (Guerdouh and Barkat, 2015)as reported by other
251 similar works. This may be attributed to the different extractants and diluents used between
252 this work and other similar works (F.Adjel and D.Barkat, 2011; Guerdouh and Barkat, 2015).
253 In this work, multiple FFAs consisting of lauric acid (49 wt%), myristic acid (17 wt%), oleic
254 acid (11 wt%), palmitic acid (10 wt%), octanoic acid (5 wt%), decanoic acid (4 wt%), and
255 stearic acid (2 wt%) (Halim et al., 2020, 2019) were used as the extractants, while a mixture
256 of kerosene (added diluent) and other minor components of PKFAD, mainly tri-, di- and
257 monoacylglycerols (Ibrahim, 2013), was employed as the diluent. Other similar works, by
258 contrast, applied lauric acid as the sole extractant and chloroform (F.Adjel and D.Barkat,
259 2011), cyclohexane (Guerdouh and Barkat, 2015), or toluene (Guerdouh and Barkat, 2015) as
260 the sole diluent. Since extractant is a ligand (Lewis base) which coordinates to a metal ion
261 (Lewis acid) via a Lewis acid-base reaction to produce a metal-extractant complex, different
262 extractants with distinct sizes, charges, and electron configurations would have a
263 considerable impact on the coordination number (Reid, 2018), and thus the stoichiometry of
264 the metal-extractant complexes formed. Different diluents, on the other hand, tend to show
265 varying degrees of intermolecular interaction with the extractant depending on their dipole
266 moments, solubility, and dielectric constant (Aksamitowski et al., 2019) and, thus, may also

affect the number of extractant molecules bound to a metal ion. Accordingly, the dissimilarities in both the extractant and diluent used between this work and other similar works (F.Adjel and D.Barkat, 2011; Guerdouh and Barkat, 2015) led to the discrepancy in the stoichiometry of Cu(II)-FFA complexes obtained. Given that the coordination numbers of Cu(II) are typically 4 and 6 (Rydberg et al., 2004), the stoichiometry of 1:6 obtained for Cu(II)-FFA complexes in this work is reasonably acceptable.

3.2 Extraction thermodynamics of Cu(II) by PKFAD

The extraction thermodynamics of Cu(II) by PKFAD was investigated over a temperature range from 25 to 70°C. In this investigation, thermodynamic parameters, namely, ΔG^o, ΔH^o, and ΔS^o due to the migration of a unit mole of Cu(II) from the aqueous to the organic phase were evaluated. The ΔG^o of Cu(II) extraction at various temperatures was calculated by (Rydberg et al., 2004):

$$\Delta G^\circ = -2.303RT \log K_{ex} \quad (9)$$

where R is the universal gas constant (8.314 J/mol.K) and T is the temperature. With a constant dimeric FFA concentration of 1.87 M and a pH_{eq} of 4.0, the values of log K_{ex} at different temperatures were determined from Eq. (5) and they were associated with ΔH^o according to the Van't Hoff equation (Rydberg et al., 2004):

$$\log K_{ex} = \frac{-\Delta H^\circ}{2.303RT} + constant \quad (10)$$

The corresponding values of ΔS^o and $-T\Delta S^o$ were then calculated by the Gibbs–Helmholtz equation (Rydberg et al., 2004):

$$\Delta S^\circ = \frac{\Delta H^\circ - \Delta G^\circ}{T} \quad (11)$$

Table 4 shows the thermodynamic data (log K_{ex}, ΔS^o, $-T\Delta S^o$, ΔG^o) obtained from Cu(II) extraction by PKFAD, with FFAs as the active components. The value of ΔH^o (-5.85 kJ/mol) was determined from the slope of a linear plot of log K_{ex} against T^{-1} (Fig. 4) based on Eq. (10). These thermodynamic data obtained reveal that the complexation reaction between Cu(II) and FFAs was accompanied by negative ΔH^o and ΔS^o, as well as positive -TΔS^o and ΔG^o. The negative ΔH^o indicates that the complexation reaction was exothermic and favored at low temperatures, as shown by the decreasing log K_{ex} with temperature in Table 4. The negative ΔS^o, on the other hand, corresponds to decreasing randomness in the system without disruption of the hydration spheres of Cu(II) (Choppin and Morgenstern, 2000; Rydberg et al., 2004). This negative ΔS^o gave rise to the positive -TΔS^o which, when coupled with the negative ΔH^o, brought about the positive ΔG^o according to Eq. (11). The positive ΔG^o implies that the complexation reaction between Cu(II) and FFAs was not energetically favorable and the reaction happened non-spontaneously within the temperature range studied.

Table 4 Thermodynamic data obtained from Cu(II) extraction by PKFAD

T (K)	log K_{ex}	ΔS^o (kJ/mol·K)	$-T\Delta S^o$ (kJ/mol)	ΔG^o (kJ/mol)
298	-8.419	-0.181	53.89	48.04
303	-8.485	-0.182	55.08	49.23
313	-8.513	-0.182	56.87	51.02
323	-8.514	-0.181	58.51	52.65
343	-8.577	-0.181	62.18	56.33

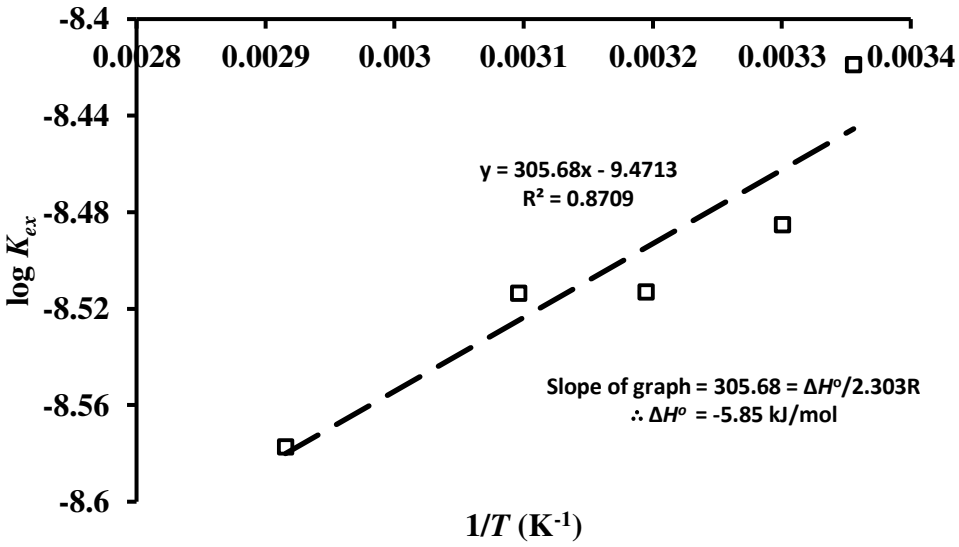

Fig. 4 log K_{ex} vs. T^{-1}

To predict the structure of either inner- or outer-sphere for Cu(II)-FFA complexes, the net ΔH^o and ΔS^o changes of the complexation reaction were examined. Since both the negative ΔH^o and ΔS^o obtained were -5.85 kJ/mol (Fig. 4) and -0.18 kJ/mol.K (Table 4), respectively, the net ΔH^o and ΔS^o changes were negative and thus suggesting an outer-sphere structure for Cu(II)-FFA complexes (Rydberg et al., 2004). These negative ΔH^o (favorable) and ΔS^o (unfavorable) attained also imply that the binding of Cu(II) to FFAs was primarily driven by enthalpy (Arisaka and Kimura, 2011) and FFAs acted as non-chelating or monodentate ligands. Several researchers have reported the similar findings for the enthalpy-driven complexation reaction (Arisaka and Kimura, 2011; Mishra and Devi, 2011; Thakare and Malkhede, 2014; Wang et al., 2018) and the outer-sphere metal-extractant complexes (Bell et al., 2008; El-Sweify et al., 2008) as this work, while others have recorded the entropy-driven reaction (Mishra and Devi, 2018; Yin et al., 2015) and the inner-sphere complexes (Arisaka and Kimura, 2011; Hu et al., 2017; Mishra and Devi, 2018). Fig. 5 illustrates the postulated outer-sphere structure of a Cu(II)-FFA complex in PKFAD based on

the thermodynamic data obtained (Table 4 and Fig. 4). The complex consists of a hydrated Cu(II) located at its center with three dimeric FFA molecules surrounding it. The hydrated Cu(II) is covalently bound to the oxygen atoms of C-OH and C=O of FFA molecules via hydrogen bonding.

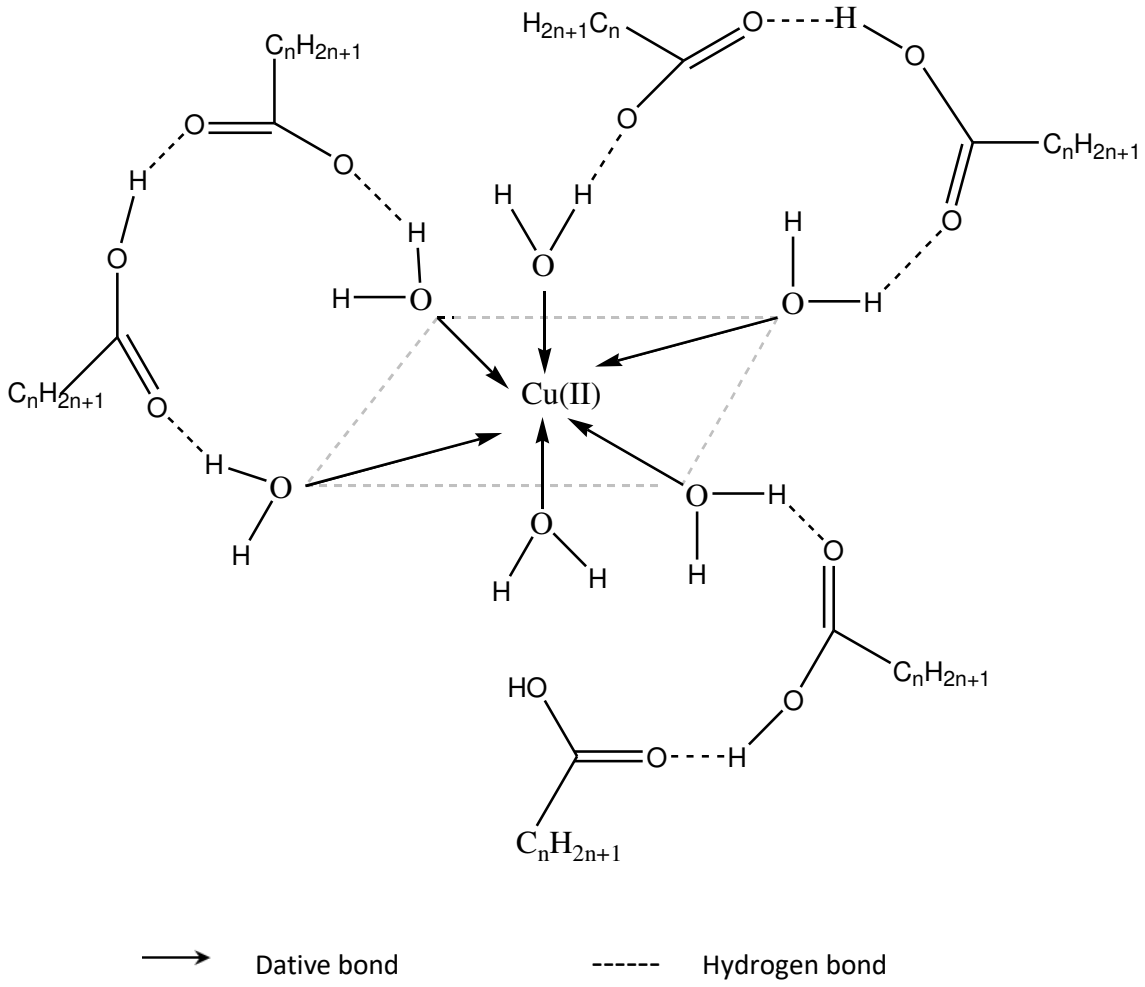

Fig. 5 Postulated outer-sphere structure of Cu(II)-FFA complex in PKFAD

3.3 FTIR analysis

To verify the presence of Cu(II)-FFA complexes in PKFAD, FTIR analysis was conducted on PKFAD samples with and without Cu(II)-FFA complexes and the spectra obtained are as shown in Fig. 6. The spectra reveal that the intensity of a strong absorption

peak at a wavelength of 1709 cm^{-1}, which is assigned to the carbonyl (C=O) stretch of a carboxylic acid (B.Stuart, 2004), is lower for the PKFAD sample with Cu(II)-FFA complexes compared to that for the PKFAD sample without Cu(II)-FFA complexes. The former indicates a smaller amount of carboxylic moieties in the PKFAD sample following the heterolytic cleavage of the O-H bonds in the carboxylic moieties at one end of the FFAs to release the acidic protons (H^+) for cation exchange with Cu(II) during the complexation reaction (Eq. 6), while the latter denotes a larger amount of carboxylic moieties in the PKFAD sample due to the absence of the complexation reaction (Eq. 6). In fact, similar results have been reported in our previous studies (Chang et al., 2011, 2010).

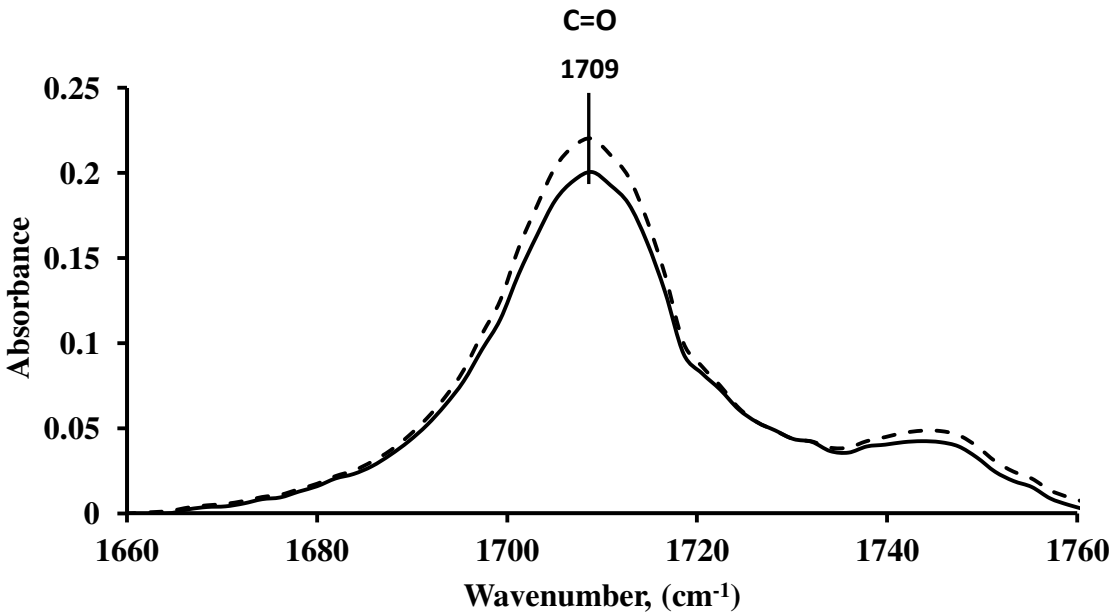

Fig. 6 FTIR spectra for PKFAD samples loaded with (—) and without (---) Cu(II)-FFA complexes

3.4 UV-Vis analysis

Fig. 7 shows the UV-Vis spectra of PKFAD before and after extraction with wavelengths in a range from 550 to 800 nm. The broad absorption band observed at a

wavelength of 679 nm (Wojciechowski et al., 2008) in the spectrum of PKFAD after extraction was caused by the presence of Cu(II)-FFA complexes, while no such band was found in the spectrum of PKFAD before extraction. The band observed at 679 nm indicates the *d-d* transition in the Cu(II)-FFA complexes, and thus suggesting an octahedral molecular geometry of the complexes as reported by Guerdouh and Barkat (Guerdouh and Barkat, 2017). This result reaffirms the presence of Cu(II)-FFA complexes in PKFAD and also supports the stoichiometry of 1:6 for Cu(II)-FFA complexes obtained earlier from both the equilibrium slope and numerical analyses.

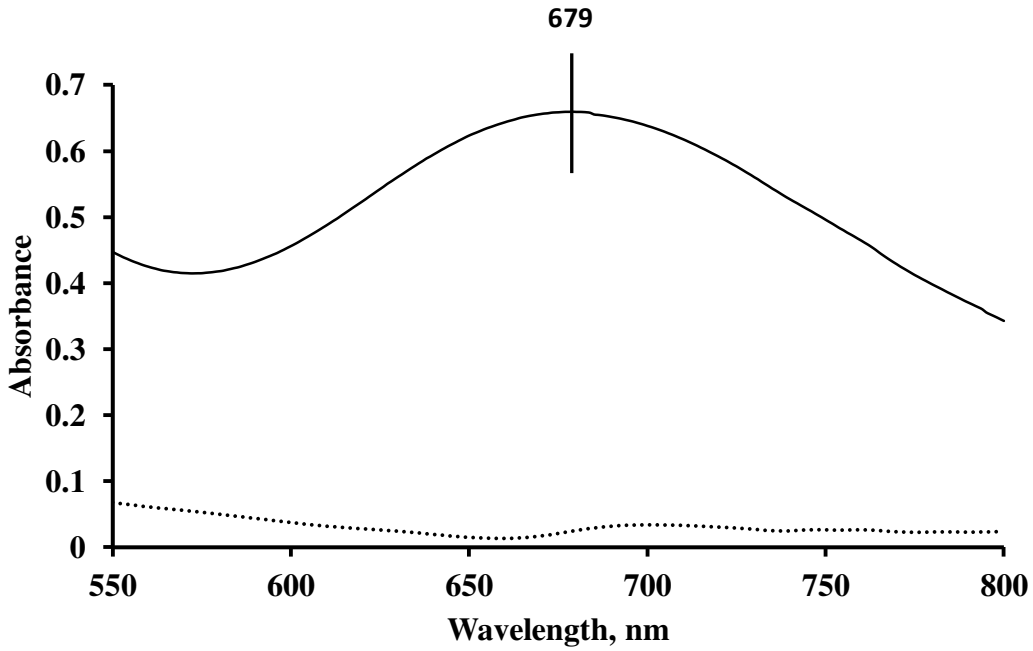

Fig 7 UV-Vis spectra of PKFAD before (⋯⋯) and after (——) extraction

4.0 Conclusions

Both the equilibrium slope and numerical analyses uncovered that one mole of Cu (II) was solvated with three moles of dimeric free fatty acids (FFAs), giving rise to a stoichiometric ratio of Cu(II) to FFA of 1:6 in the formation of Cu(II)-FFA complexes

(extracted species) in palm kernel fatty acid distillate (PKFAD). The thermodynamic study demonstrated that the complexation reaction between Cu(II) and FFAs was accompanied by negative standard enthalpy change (ΔH^o) and standard entropy change (ΔS^o), as well as positive standard Gibbs free energy change (ΔG^o). These thermodynamic data obtained implied that the complexation reaction between Cu(II) and FFAs was exothermic, nonspontaneous, and enthalpy-driven over the temperature range studied. An outer-sphere structure for Cu(II)-FFA complexes in PKFAD was proposed based on the negative net ΔH^o and ΔS^o changes attained.

Declarations

Ethics approval and consent to participate

Not applicable.

Consent for publication

Not applicable.

Availability of data and materials

The datasets used and/or analysed during the current study are available from the corresponding author on reasonable request.

Competing interests

No competing interests in financial and personal relationships.

Funding

Ministry of Education, Malaysia under the Fundamental Research Grant Scheme (FRGS/1/2019/TK10/UITM/02/9).

Authors' contributions

Siti Fatimah Abdul Halim: conceptualization, investigation, methodology, data collection, data analysis, writing- original draft preparation.

Siu Hua Chang: Writing- original draft preparation, reviewing and editing, supervision.

Norhashimah Morad: supervision.

Acknowledgements

This work was supported by the Ministry of Education, Malaysia under the Fundamental Research Grant Scheme (FRGS/1/2019/TK10/UITM/02/9).

References

Aidi, A., Barkat, D., 2018. Thermodynamics of the extraction of Cu(II) with capric acid in cyclohexane. Courrier du Savoir 26, 23–28.

Aidi, A., Barkat, D., 2010. Solvent extraction of copper(II) from sulfate medium with N -(2-hydroxybenzylidene)aniline. Journal of Coordination Chemistry 63, 4136–4144. https://doi.org/10.1080/00958972.2010.530662

Aksamitowski, P., Filipowiak, K., Wieszczycka, K., 2019. Selective extraction of copper from Cu-Zn sulfate media by new generation extractants. Separation and Purification Technology 222, 22–29. https://doi.org/10.1016/j.seppur.2019.03.100

Arisaka, M., Kimura, T., 2011. Thermodynamic and spectroscopic studies on Am(III) and Eu(III) in the extraction system of N,N,N',N'-Tetraoctyl-3-Oxapentane-1,5-Diamide in n-Dodecane/nitric acid. Solvent Extraction and Ion Exchange 29, 72–85. https://doi.org/10.1080/07366299.2011.539127

B.Stuart, 2004. Infrared Spectroscopy: Fundamentals and Applications. John Wiley & Sons, Inc., The United Kingdom.

Bar, D.E., Barkat, D., 2016. A statistical approach to the experimental of the leaching of sulfide copper from the ores using lixiviant sulfuric acid. Journal of Mining Science 52, 569–575. https://doi.org/10.1134/S1062739116030849

Bell, K.J., Westra, A.N., Warr, R.J., Chartres, J., Ellis, R., Tong, C.C., Blake, A.J., Tasker, P.A., Schröder, M., 2008. Outer-sphere coordination chemistry: Selective extraction and

427 transport of the [PtCl6]2- anion. Angewandte Chemie - International Edition 47, 1745–
428 1748. https://doi.org/10.1002/anie.200703272
429 Benalia, H., Barkat, D., 2020. Solvent extraction studies of nickel(II) by capric acid from
430 sodium sulfate solution. Chemical Engineering Communications 207, 306–318.
431 https://doi.org/10.1080/00986445.2019.1588730
432 Chang, S.H., 2020. Utilization of green organic solvents in solvent extraction and liquid
433 membrane for sustainable wastewater treatment and resource recovery—A review.
434 Environmental Science and Pollution Research 27, 32371–32388.
435 https://doi.org/10.1007/s11356-020-09639-7
436 Chang, S.H., 2018. A comparative study of batch and continuous bulk liquid membranes in
437 the removal and recovery of Cu(II) ions from wastewater. Water Air Soil Pollut 229, 1–
438 11. https://doi.org/https://doi.org/10.1007/s11270-017-3659-z A
439 Chang, S.H., Teng, T.T., Ismail, N., 2011. Efficiency, stoichiometry and structural studies of
440 Cu(II) removal from aqueous solutions using di-2-ethylhexylphosphoric acid and
441 tributylphosphate diluted in soybean oil. Chemical Engineering Journal 166, 249–255.
442 https://doi.org/10.1016/j.cej.2010.10.069
443 Chang, S.H., Teng, T.T., Ismail, N., 2010. Extraction of Cu(II) from aqueous solutions by
444 vegetable oil-based organic solvents. Journal of Hazardous Materials 181, 868–872.
445 https://doi.org/10.1016/j.jhazmat.2010.05.093
446 Choppin, G.R., Morgenstern, A., 2000. Thermodynamics of solvent extraction. Solvent
447 Extraction and Ion Exchange 18, 1029–1049.
448 https://doi.org/10.1080/07366290008934721
449 El-Sweify, F.H., Abdel-Fattah, A.A., Ali, S.M., 2008. Extraction thermodynamics of Th(IV)
450 in various aqueous organic systems. Journal of Chemical Thermodynamics 40, 798–805.
451 https://doi.org/10.1016/j.jct.2008.01.013

Elizalde, M.P., Rua, M.S., Menoyo, B., Ocio, A., 2019. Solvent extraction of copper from acidic chloride solutions with LIX 84. Hydrometallurgy 183, 213–220. https://doi.org/10.1016/j.hydromet.2018.12.013

F.Adjel, D.Barkat, 2011. Synergistic extraction of copper(II) from sulfate medium with capric acid and tri-n-octylphosphine oxide in chloroform. Journal of Coordination Chemistry 64, 574–582. https://doi.org/10.1080/00958972.2010.551400

Ghosh, A., Datta, D., Uslu, H., Bamufleh, H.S., Kumar, S., 2018. Separation of copper ion (Cu) from aqueous solution using tri-n-butyl phosphate and di-2-ethylhexyl phosphoric acid as extractants. Journal of Molecular Liquids 258, 147–154. https://doi.org/10.1016/j.molliq.2018.03.007

Gopi Kiran, M., Pakshirajan, K., Das, G., 2017. An overview of sulfidogenic biological reactors for the simultaneous treatment of sulfate and heavy metal rich wastewater. Chemical Engineering Science 158, 606–620. https://doi.org/10.1016/j.ces.2016.11.002

Guerdouh, A., Barkat, D., 2017. Influence of the solvent on the extraction of copper(II) from nitrate medium using salicylideneaniline. Journal of Dispersion Science and Technology 38, 930–934. https://doi.org/10.1080/01932691.2016.1215926

Guerdouh, A., Barkat, D., 2015. Solvent effects on the extraction of copper(II) with lauric acid. Journal of Thermodynamics & Catalysis 6, 1–7. https://doi.org/10.4172/2157-7544.1000148

Halim, S.F.A., Chang, S.H., Morad, N., 2020. Extraction of Cu (II) ions from aqueous solutions by free fatty acid-rich oils as green extractants. Journal of Water Process Engineering 33, 100997. https://doi.org/10.1016/j.jwpe.2019.100997

Halim, S.F.A., Chang, S.H., Morad, N., 2019. Parametric studies of Cu (II) ion extraction into palm kernel fatty acid distillate as a green organic solvent. Journal of Environmental Chemical Engineering 7, 103488. https://doi.org/10.1016/j.jece.2019.103488

Hu, F., Hu, H., Hu, J., Zhu, S., Yang, J., Wang, Y., 2017. Improving selective separation of Cu (II) from acidic polymetallic media with 2-ethylhexyl 4-pyridinecarboxylate ester : Extraction behaviors , coordination structure and microscopic mechanism. Journal of Molecular Liquids 248, 1050–1058. https://doi.org/10.1016/j.molliq.2017.10.143

Hu, F., Hu, H., Luo, Y., Wang, Y., Yang, J., Hu, J., 2018. The separation of Ni(II) over base metal ions in acidic polymetallic medium: Synergistic extraction and structural evidence. Hydrometallurgy 181, 240–247. https://doi.org/10.1016/j.hydromet.2018.10.007

Ibrahim, N.A., 2013. Characteristics of malaysian palm kernel and its products. Journal of Oil Palm Research 25, 245–252.

Jafari, H., Abdollahi, H., Gharabaghi, M., Balesini, A.A., 2018. Solvent extraction of zinc from synthetic Zn-Cd-Mn chloride solution using D2EHPA: Optimization and thermodynamic studies. Separation and Purification Technology 197, 210–219. https://doi.org/10.1016/j.seppur.2018.01.020

Michels, H.T., Moran, W., Michel, J., 2008. Antimicrobial properties of copper alloy surfaces. Advanced Materials and Processes 166, 57–58.

Mishra, B.B., Devi, N., 2018. Solvent extraction and separation of europium (III) using a phosphonium ionic liquid and an organophosphorus extractant-A comparative study. Journal of Molecular Liquids 271, 389–396. https://doi.org/10.1016/j.molliq.2018.08.160

Mishra, S., Devi, N., 2011. Extraction of copper(II) from hydrochloric acid solution by Cyanex 921. Hydrometallurgy 107, 29–33. https://doi.org/10.1016/j.hydromet.2010.12.016

Myers, R.H., Montgomery, D.C., M.Anderson-Cook, C., 2016. Response surface methodology, 4th. ed. ed. John Wiley & Sons Inc, New Jersey.

Razavi, S.M., Haghtalab, A., Khanchi, A.R., 2018. Thermodynamic modeling of the solvent extraction equilibrium for the recovery of vanadium (V) from acidic sulfate solutions using Di-(2-ethylhexyl) phosphoric acid. Fluid Phase Equilibria 474, 20–31. https://doi.org/10.1016/j.fluid.2018.07.007

Reid, R., 2018. Inorganic Chemistry. ED Tech Press, United Kingdom.

Rydberg, J., Micheal, C., Musikas, C., R.Choppin, G., 2004. Solvent extracion principles and practice, 2nd. ed. ed. Marcel Dekker Inc, United States of America.

Sulaiman, R.N.R., Othman, N., 2018. Solvent extraction of nickel ions from electroless nickel plating wastewater using synergistic green binary mixture of D2EHPA-octanol system. Journal of Environmental Chemical Engineering 6, 1814–1820. https://doi.org/10.1016/j.jece.2018.02.035

Thakare, Y.S., Malkhede, D.D., 2014. Solvent Extraction and Separation of Gallium(III) using Hexaacetato Calix(6)Arene. Separation Science and Technology (Philadelphia) 49, 1198–1207. https://doi.org/10.1080/01496395.2013.872657

Tsivintzelis, I., Kontogeorgis, G.M., Panayiotou, C., 2017. Dimerization of Carboxylic Acids : An Equation of State Approach. The Journal of physical chemistry B 121, 2153–2163. https://doi.org/10.1021/acs.jpcb.6b10652

Wahab, A.A.A., Chang, S.H., Som, A.M., 2016. Stoichiometry of Cu(II) ion extraction with di-2-ethylhexylphosphoric acid dissolved in waste palm cooking oil. International Journal of Technology 5, 530–537. https://doi.org/10.14716/ijtech.v7i5.3292

Wang, S., 2007. Aqueous lixiviants: Principle, types, and applications. Jom 59, 37–42. https://doi.org/10.1007/s11837-007-0129-x

Wang, Y., Zhang, Z., Kuang, S., Wu, G., Li, Yanling, Li, Yunhui, Liao, W., 2018. Selective extraction and recovery of copper from chloride solution using Cextrant 230. Hydrometallurgy 181, 16–20. https://doi.org/10.1016/j.hydromet.2018.08.007

527 Wilson, A.M., Bailey, P.J., Tasker, P.A., Turkington, J.R., Grant, R.A., Love, J.B., 2014.
528 Solvent extraction: the coordination chemistry behind extractive metallurgy. Chem. Soc.
529 Rev. 43, 123–134. https://doi.org/10.1039/C3CS60275C
530 Wojciechowski, K., Kucharek, M., Buffle, J., 2008. Mechanism of Cu(II) transport through
531 permeation liquid membranes using azacrown ether and fatty acid as carrier. Journal of
532 Membrane Science 314, 152–162. https://doi.org/10.1016/j.memsci.2008.01.036
533 Yin, S.H., Li, S.W., Xie, F., Zhang, L.B., Peng, J.H., 2015. Study on the aqueous solution
534 behavior and extraction mechanism of Nd(III) in the presence of the complexing agent
535 lactic acid with di-(2-ethylhexyl) phosphoric acid. RSC Advances 5, 64550–64556.
536 https://doi.org/10.1039/c5ra09928e
537

Figures

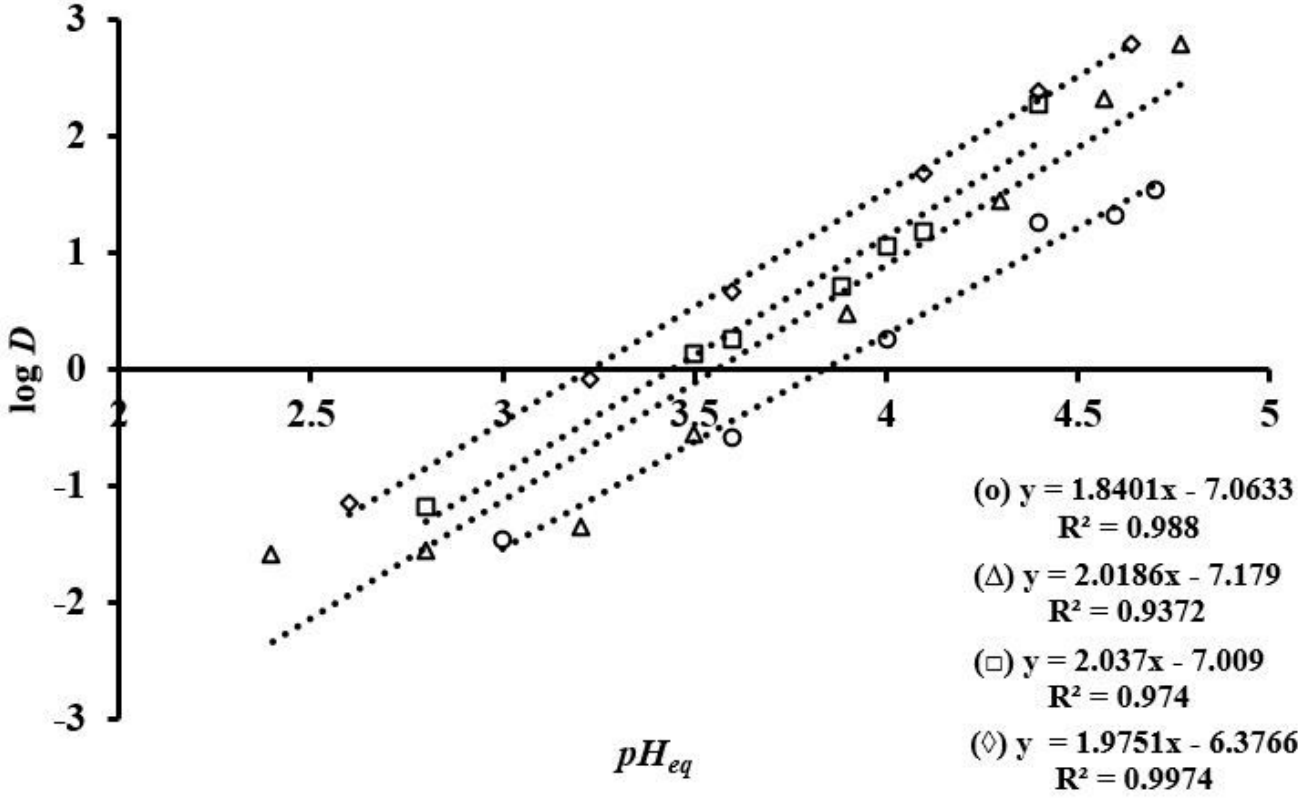

Figure 1

log D vs. pHeq at different initial Cu(II) concentrations (20 mg/L (□),100mg/L (Δ), 300 mg/L (□) and 500 mg/L(◊)

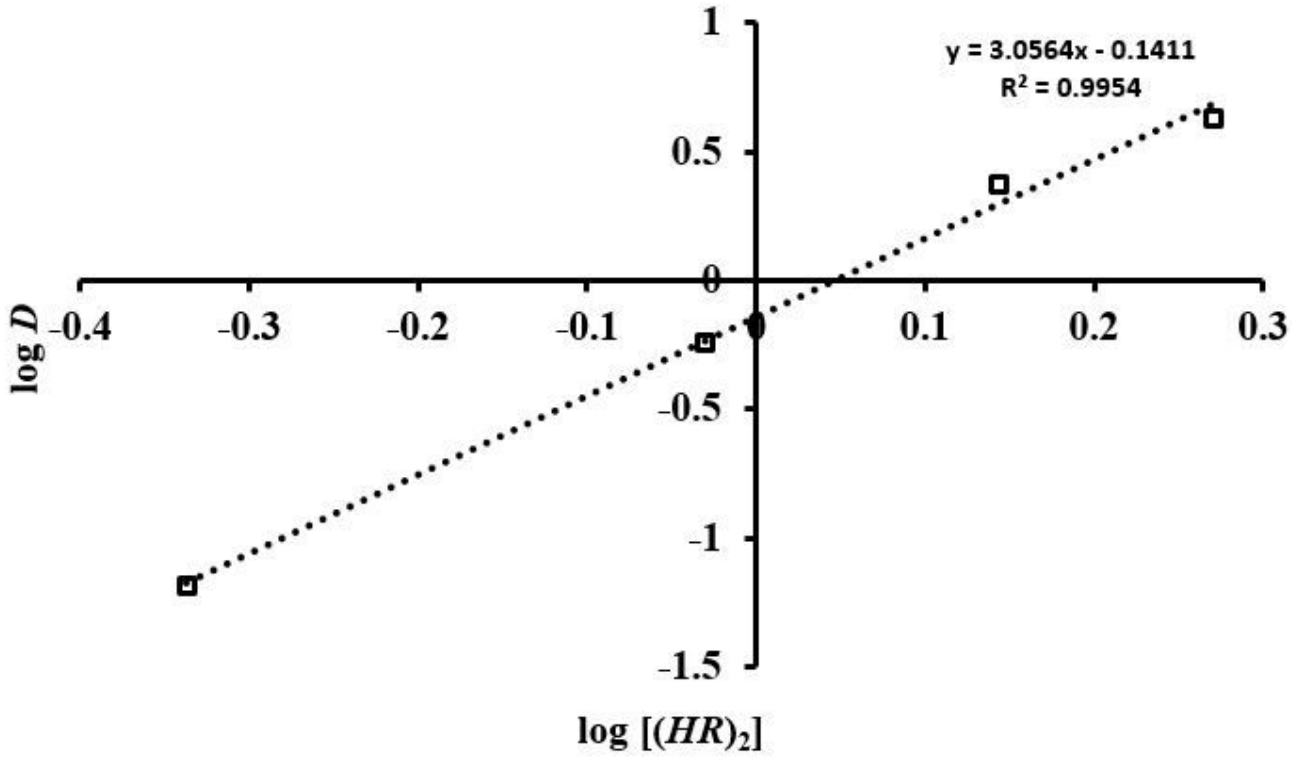

Figure 2

log D vs. log [(HR)2] at initial Cu(II) concentration of 100 mg/L and pHeq of 4.0

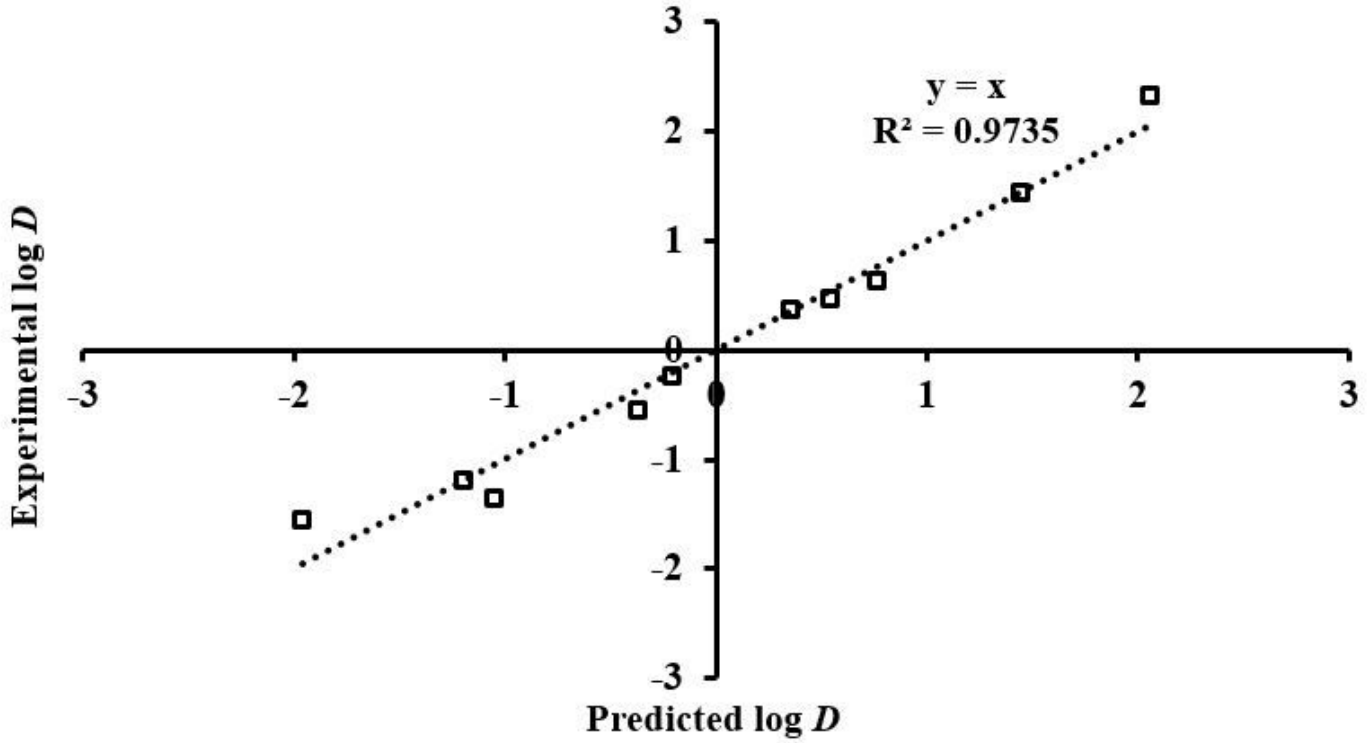

Figure 3

Experimental log D vs. predicted log D

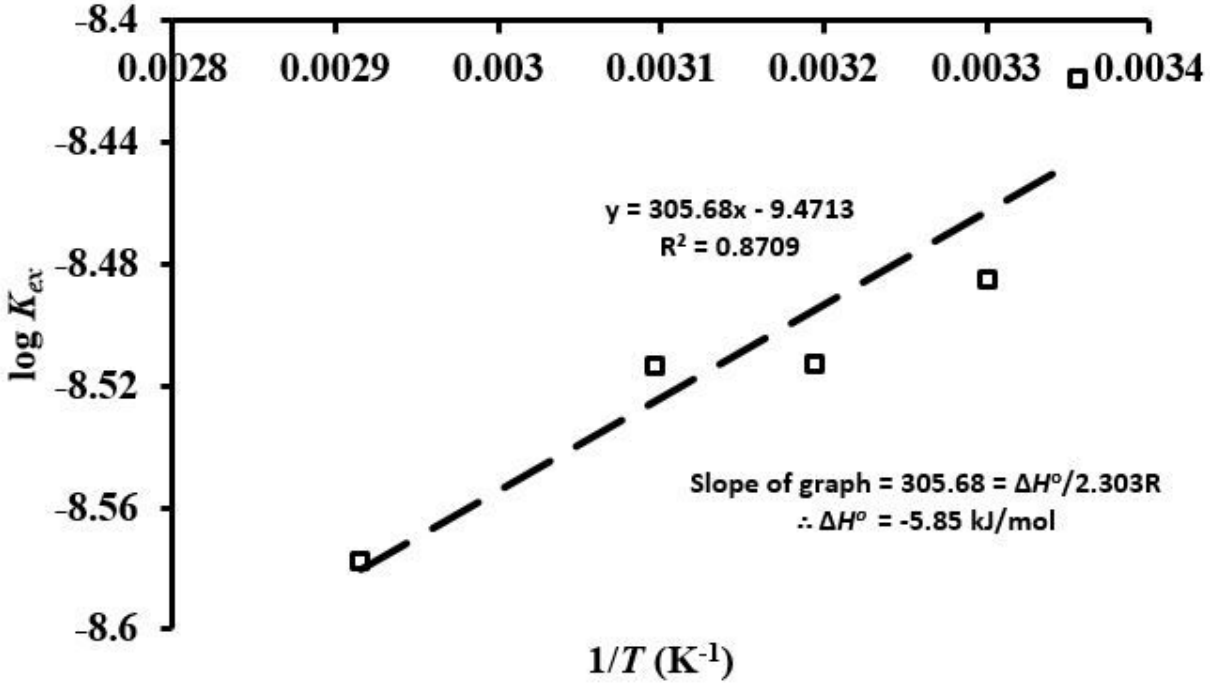

Figure 4

log Kex vs. T-1

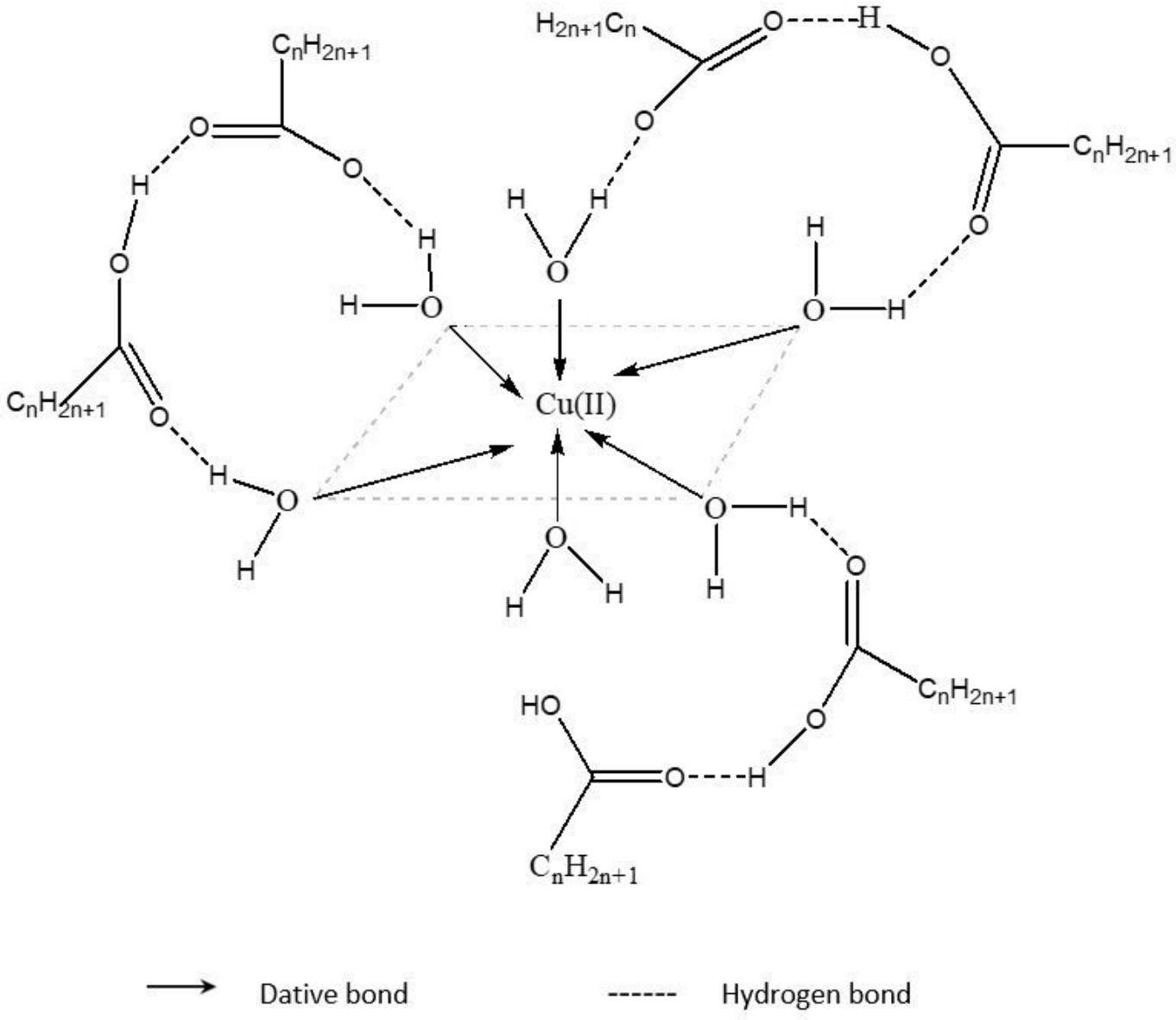

Figure 5

Postulated outer-sphere structure of Cu(II)-FFA complex in PKFAD

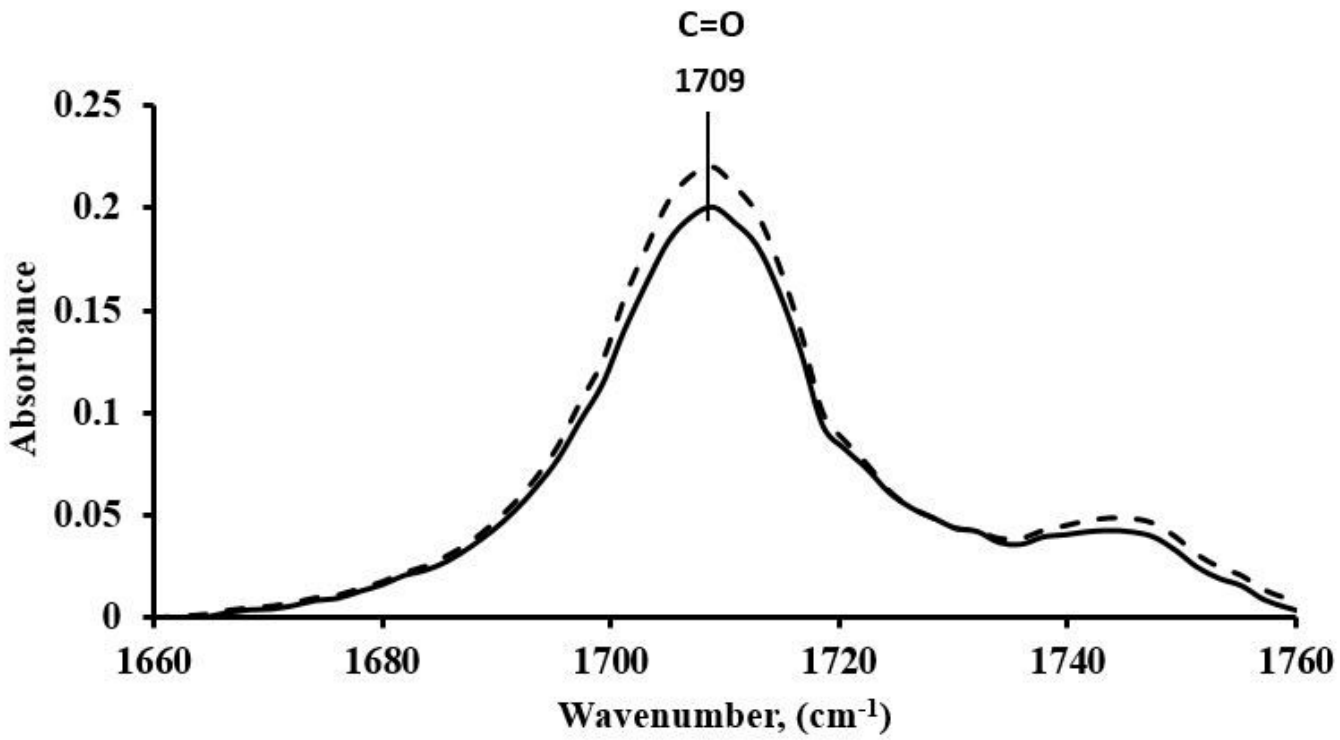

Figure 6

FTIR spectra for PKFAD samples loaded with (___) and without (---) Cu(II)-FFA complexes

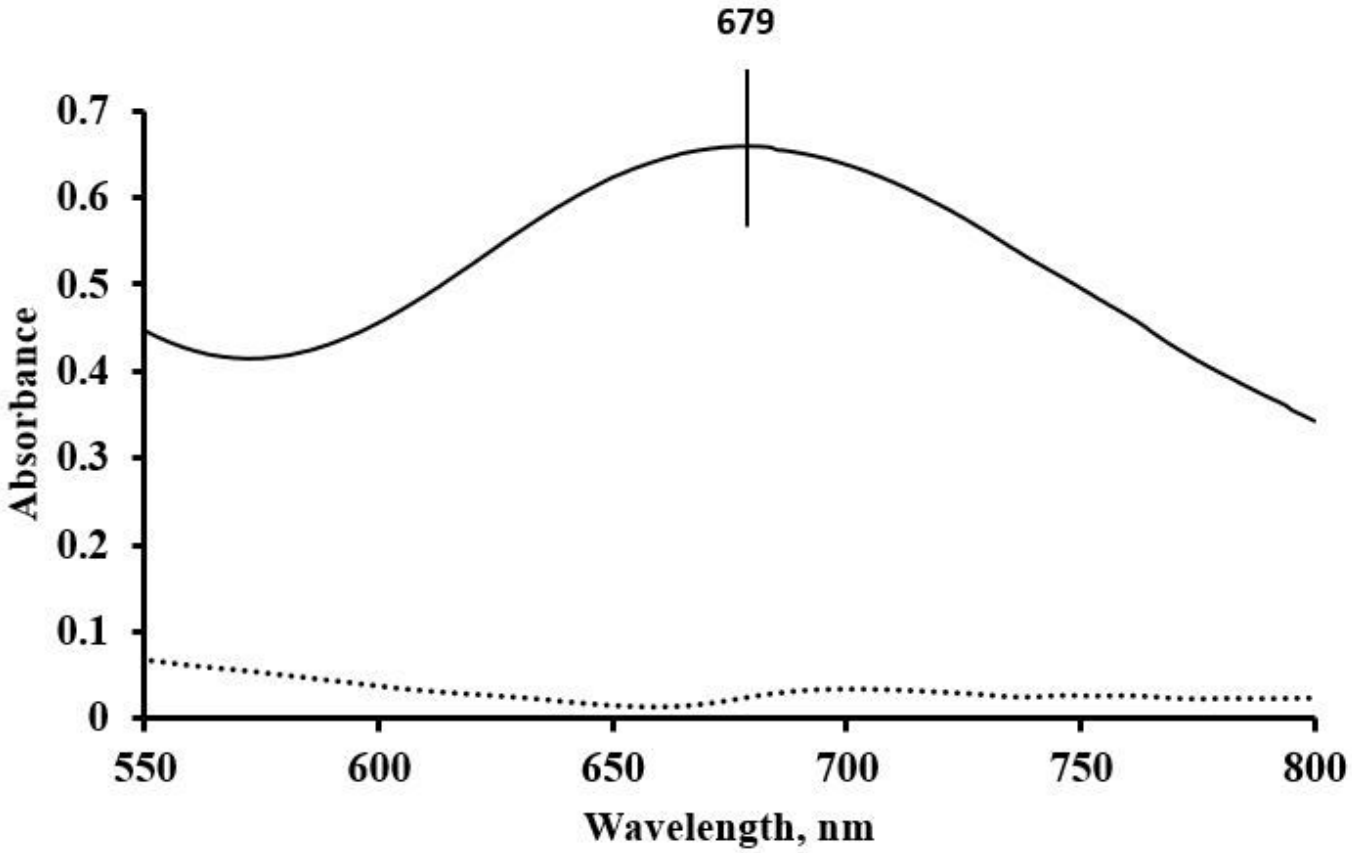

Figure 7

UV-Vis spectra of PKFAD before (.....) and after (▯▯) extraction